

# The role of platelets in thrombus fibrosis and vessel wall remodeling after venous thrombosis

Elise DeRoo<sup>1,2</sup>  | Kimberly Martinod<sup>1,2</sup>  | Deya Cherpokova<sup>1,2</sup> | Tobias Fuchs<sup>1,2</sup> | Stephen Cifuni<sup>1,2</sup> | Long Chu<sup>1,2</sup> | Caleb Staudinger<sup>1,2</sup> | Denisa D. Wagner<sup>1,2,3</sup> 

<sup>1</sup>Program in Cellular and Molecular Medicine, Boston Children's Hospital, Boston, MA, USA

<sup>2</sup>Department of Pediatrics, Harvard Medical School, Boston, MA, USA

<sup>3</sup>Division of Hematology/Oncology, Boston Children's Hospital, Boston, MA, USA

## Correspondence

Denisa D. Wagner, Program in Cellular and Molecular Medicine, Boston Children's Hospital, Harvard Medical School, 1 Blackfan Circle, 9th Floor, Boston, MA 02115, USA.  
Email: denisa.wagner@childrens.harvard.edu

## Present address

Elise DeRoo, Department of Surgery, University of Wisconsin Vascular Surgery Division, University of Wisconsin Hospitals and Clinics, Madison, WI, USA

Kimberly Martinod, Department of Cardiovascular Sciences, Center for Molecular and Vascular Biology, KU Leuven, Leuven, Belgium

Deya Cherpokova, CSL Behring GmbH, Marburg, Germany  
Stephen Cifuni, Sanofi/Genzyme, Middleton, MA, USA

## Funding information

American Society of Hematology; National Heart, Lung, and Blood Institute, Grant/Award Number: R35 HL135765; American Heart Association; Society for Vascular Surgery

## Abstract

**Purpose:** Platelets are known to play an important role in venous thrombogenesis, but their role in thrombus maturation, resolution, and postthrombotic vein wall remodeling is unclear. The purpose of this study was to determine the role that circulating platelets play in the later phases of venous thrombosis.

**Methods:** We used a murine inferior vena cava (IVC) stenosis model. Baseline studies in untreated mice were performed to determine an optimal postthrombotic time point for tissue harvest that would capture both thrombus maturation/resolution and postthrombotic vein wall remodeling. This time point was found to be postoperative day 10. After undergoing IVC ultrasound on day 2 to confirm venous thrombus formation, mice were treated with a daily injection of platelet-depleting antibody (anti-GP1b $\alpha$ ) to maintain thrombocytopenia or with control IgG until postoperative day 10, at which time IVC and thrombi were harvested and thrombus length, volume, fibrosis, neovascularization, and smooth muscle cell invasion analyzed. Vein wall fibrosis and intimal thickening were also determined.

**Results:** Mice that were made thrombocytopenic after venous thrombogenesis had thrombi that were less fibrotic, with fewer invading smooth muscle cells. Furthermore, thrombocytopenia in the setting of venous thrombosis resulted in less postthrombotic vein wall intimal thickening. Thrombus volume did not differ between thrombocytopenic mice and their control peers.

**Conclusions:** This work suggests that circulating platelets contribute to venous thrombus maturation, fibrosis, and adverse vein wall remodeling, and that that inhibition of platelet recruitment may decrease thrombus and vein wall fibrosis, thus helping thrombolysis and preventing postthrombotic syndrome.

## KEYWORDS

fibrosis, platelets, post-thrombotic syndrome, vascular remodeling, venous thrombosis

## 1 | INTRODUCTION

Venous thromboembolism (VTE) is a relatively common disease, with an estimated incidence of 300 000 to 600 000 events in the United States annually.<sup>1</sup> Venous thromboembolism recurs in approximately 30% of patients within 10 years after an event and is associated with not only reduced survival, but also significant morbidity and substantial health care costs, with an estimated \$7 to \$10 billion spent annually in the treatment of acute VTE and its complications.<sup>1</sup>

Currently, anticoagulation remains a mainstay of treatment for patients with deep vein thrombosis (DVT).<sup>2</sup> Anticoagulation prevents DVT extension, but does not significantly accelerate thrombus lysis.<sup>3</sup> Pharmacomechanical thrombolysis can accelerate DVT lysis, but it can only be used in a select subset of patients and is associated with significant bleeding risks.<sup>4,5</sup> Between 20% and 60% of those who experience DVT go on to develop chronic leg pain, swelling, redness, and ulcers, a collection of symptoms known as postthrombotic syndrome (PTS).<sup>1,6</sup> At the anatomic level, PTS is associated with venous valve destruction leading to reflux, venous outflow obstruction, and decreased venous compliance, characterized at the histologic level by vein wall (VW) thickening, fibrosis, and neointimal thickening.<sup>6-10</sup> Studies have shown slow thrombus resolution to be a predictor of PTS development.<sup>3,11</sup> With no effective treatments for PTS after its onset, efforts should be focused on PTS prevention.<sup>12</sup> Although the pathophysiology underlying PTS is incompletely understood, thrombus remodeling and the process of vein recanalization are thought to contribute to its development.<sup>13</sup> Therefore, there continues to be a need for research that focuses on the mechanisms underlying thrombus maturation, resolution, and VW remodeling.

Thrombus resolution is a complex process, not dissimilar to wound healing, involving the influx of inflammatory cells, smooth muscle cells, and fibroblasts, followed by thrombus fibrosis, retraction, fibrinolysis, and neovascularization.<sup>14-24</sup> As thrombi resolve, the injury to the VW conferred by the thrombus becomes evident.<sup>6,8,9</sup> Points of anchoring between the thrombus and the VW appear to serve as a bridge for invading endothelial cells, fibroblasts, and smooth muscle cells, allowing for thrombus maturation, but these also tend to be areas of high VW fibrosis and intimal thickening.<sup>14,15</sup> The importance of neutrophil and monocyte invasion to timely thrombus resolution is well established, but the role of other circulating cells and blood components remains unclear.<sup>9,19,25,26</sup>

Platelets are rich in both pro- and anti-angiogenic factors, as well as transforming growth factor  $\beta$  (TGF- $\beta$ ), a known driver of tissue fibrosis, and PAI-1, an inhibitor of fibrinolysis.<sup>27-30</sup> Studies have shown that, on balance, platelets tend to be pro-angiogenic and play a critical role in both driving and supporting normal angiogenesis both in vitro and in vivo.<sup>30-34</sup> These findings suggested that platelets may play an important, yet underappreciated, role in thrombus maturation.

The purpose of this study was to determine, using a mouse model of DVT known to produce thrombi structurally similar to

### Essentials

- Venous thrombosis (VT) is associated with high morbidity and mortality.
- Mature, fibrotic venous thrombi are more resistant to thrombolysis.
- Platelet depletion decreases thrombus fibrosis and vein wall intimal thickness.
- Circulating platelets contribute to adverse thrombus and vein wall remodeling.

human venous thrombi, whether or not platelet depletion after thrombogenesis would alter thrombus maturation, resolution, and postthrombotic VW remodeling.<sup>35</sup> Specifically, we sought to evaluate the role of platelet depletion on thrombus fibrosis and neovascularization, in addition to VW thickening, fibrosis, and intimal thickening.

## 2 | METHODS

### 2.1 | Mice

Eight- to 10-week-old C57BL/6J male mice were used for all studies. Mice were purchased from Jackson Laboratory (Bar Harbor, ME). Thirty mice were operated on in studies to determine the natural time-course of DVT resolution (2-day harvest  $n = 10$  [7/10 thrombus bearing], 8-day harvest  $n = 10$  [8/10 thrombus bearing], 16-day harvest  $n = 10$  [8/10 thrombus bearing]). A total of 45 mice were operated on in studies to determine the role of platelets in DVT resolution, with 34/45 mice developing thrombi. Of thrombi-bearing mice, two died in the perioperative period. Only thrombi that could be size matched before initiation of control treatment or platelet depletion were included, leading to  $n = 14$  mice allocated to the control group and  $n = 16$  mice allocated to the platelet depletion group.

### 2.2 | Pre-/postoperative blood tests

Twenty-four hours before surgery and 24 hours after inferior vena cava (IVC) stenosis, mice underwent blood testing to analyze platelet count. Studies in our laboratory have shown that a ~30% reduction in baseline platelet count is highly predictive of IVC thrombus formation.<sup>36</sup> All blood was collected from the retro-orbital sinus using a 25- $\mu$ L ethylenediaminetetraacetic acid-coated capillary tube. Platelet counts in wild-type (WT), untreated mice were determined using a Drew Scientific HemaVet. Platelet counts in platelet depleted or control IgG treated mice were determined using the Leukocheck (Biomedical Polymers, Inc BMP-LUKCHK-50) platelet count system.

## 2.3 | IVC stenosis surgery

Mice were anesthetized with 3.5% isoflurane and anesthesia maintained at 2% in 100% oxygen. A midline laparotomy was performed, and the IVC was exposed. Side branches between the renal and iliac veins were ligated with 7/0 polypropylene suture. A 30-G spacer was placed parallel to the IVC, and a 7/0 polypropylene suture was used to partially ligate the IVC to 10% of its original diameter. The spacer was removed, and the mouse was closed in a layered fashion. All mice were given buprenorphine (0.1 mg/kg) subcutaneously as an analgesic immediately before surgery and every 12 hours for 72 hours following surgery.

## 2.4 | Ultrasound

At 48 hours postoperatively, mice underwent IVC ultrasound (Vevo 2100) to determine (a) the incidence of thrombus formation and (b) thrombus size (length, average width, and volume). Mice were anesthetized with 3.5% isoflurane and anesthesia maintained at 2% in 100% oxygen. The IVC was visualized with a small-animal ultrasound probe and examined in transverse and sagittal views from the renal veins to the iliac bifurcation. Thrombus volume was calculated from thrombus length and average width, assuming the thrombus to be a cylinder (Vascular Analysis Package).

## 2.5 | Platelet depletion with anti-GP1b $\alpha$ antibody

Mice with IVC thrombi at postoperative day 2, as determined by ultrasound visualization, were treated with a platelet-depleting antibody (2  $\mu$ g/g, GP1b $\alpha$  antibody, Emfret Analytics, R300) or control IgG (2  $\mu$ g/g control IgG antibody, Emfret Analytics, R301) diluted in sterile saline. Mice without thrombi were excluded. Platelet-depleting and control antibodies were tested and found to be endotoxin free. Platelet counts were monitored manually using the Leukocheck platelet count system. Blood was collected from the retro-orbital sinus using a 25- $\mu$ L ethylenediaminetetraacetic acid-coated capillary tube, diluted in Leukocheck RBC lysis buffer, and examined on a Neubauer chamber at 400 $\times$  magnification to determine platelet count. All platelet counts were performed within 3 hours of blood collection.

## 2.6 | Tissue harvest

Tissue samples were harvested from WT, untreated mice at 2, 8, or 16 days postoperatively and from WT platelet-depleted or WT control-treated mice at 10 days postoperatively. At time of harvest, mice were anesthetized with isoflurane and the IVCs were exposed to allow for collection of the IVC VW and thrombi formed within the IVC. IVC, thrombus, and aorta were harvested en bloc at the level of infrarenal ligature (superior boundary) and iliac bifurcation (inferior boundary). Thrombus length was measured at time of harvest.

Because these studies were histology based, thrombus length and volume were determined on specimens to be used for histology. The IVC is translucent enough at harvest that thrombus length can be determined. Tissue samples were either embedded in optimal cutting temperature compound and frozen or fixed in 10% neutral buffered formalin for 24 hours and, subsequently, paraffin embedded for sectioning.

## 2.7 | Histologic staining

### 2.7.1 | Formalin-fixed paraffin embedded (FFPE) tissue

Tissue was formalin (10%) fixed for 24 hours, washed, dehydrated, and paraffin-embedded for further processing. Thrombus samples were serially cross-sectioned throughout the length of the thrombus. Sections taken at 400- $\mu$ m intervals were deparaffinized with graded xylene and ethanol, rehydrated in water, and stained with Masson's Trichrome Stain (Sigma-Aldrich, HT15), Elastic Van Gieson stain (Millipore, 115974), or Alizarin Red, per the manufacturer instructions. Trichrome stain was performed for VW and thrombus collagen analysis. Elastic Van Gieson stain was performed to determine VW intimal thickness. Alizarin Red stain was performed to analyze thrombus and vein-wall calcification.

### 2.7.2 | Frozen tissue

Tissue was embedded in optimal cutting temperature compound, frozen on dry ice, and stored at  $-80^{\circ}\text{C}$  until further processing. Thrombus samples were serially cross-sectioned throughout the length of the thrombus. Tissue samples at 400- $\mu$ m intervals were hematoxylin and eosin-stained or immunostained with the following primary antibodies: anti-CD31 (BD Pharmingen, 550274, 1:600); anti-VWF (DAKO, A0082, 1:800); anti-alpha smooth muscle actin (Abcam, ab5694, 1:200). Tissue samples were subsequently stained with the following secondary antibodies: AlexaFluor 488 donkey anti-Rat (Thermo Fischer Scientific, A21208, 1:1000) or AlexaFluor 568 donkey anti-Rabbit (Thermo Fischer Scientific, A10042, 1:1000).

## 2.8 | Image analysis

Images were acquired using a Zeiss Axioplan microscope in conjunction with a Zeiss AxioCam HR camera and Axiovision software.

### 2.8.1 | Thrombus volume measurement

Harvest thrombus volume ( $\mu\text{m}^3$ ) was calculated using thrombus length and average thrombus cross-sectional area, assuming the

thrombus to be a cylinder ( $V = \text{average cross-sectional area} \times L$ ). Average thrombus cross-sectional area was measured using serially sectioned, trichrome-stained FFPE sections and hematoxylin and eosin-stained frozen sections. ImageJ software was used to measure the thrombus cross-sectional area ( $\mu\text{m}^2$ ).

### 2.8.2 | Vein wall/thrombus collagen and vein wall/thrombus area measurement

Formalin-fixed paraffin embedded IVC/thrombus samples were cross-sectioned at 400- $\mu\text{m}$  intervals throughout the length of the IVC and stained with Masson's Trichrome (Sigma Aldrich). Images of each stained cross section were captured at 40 $\times$  magnification, allowing for visualization of the entire circumference of the IVC, thrombus, and surrounding tissue. ImageJ software was used to calculate the total VW area ( $\mu\text{m}^2$ ). The Threshold Color plugin was used to select for collagen stained areas and, subsequently, used to determine the total VW area occupied by collagen ( $\mu\text{m}^2$ ). The same methods were used to determine the total thrombus cross-sectional area ( $\mu\text{m}^2$ ) and intrathrombus collagen content ( $\mu\text{m}^2$ ). All images for each individual study were acquired under the same exposure conditions and were subject to the same color threshold parameters.

### 2.8.3 | Intimal thickness measurement

Formalin-fixed paraffin embedded IVC/thrombus samples were cross sectioned at 400- $\mu\text{m}$  intervals throughout the length of the IVC and stained with Elastic Tissue Van Gieson stain (Millipore). Images of the VW in all four quadrants around the lumen were captured at 400 $\times$  magnification. ImageJ software was used to measure the intimal thickness in each 400 $\times$  image: three measurements of intimal thickness were taken per image, for a total of 12 intimal measurements per cross section. Average intimal thickness was calculated for each thrombus-bearing mouse (Figure S1).

### 2.8.4 | Quantification of thrombus neovascularization and smooth muscle cell invasion

Frozen IVC/thrombus samples were cross sectioned at 400- $\mu\text{m}$  intervals throughout the length of the IVC and costained with rat anti-CD31 and rabbit anti-VWF or anti-smooth muscle actin primary antibodies. To visualize CD31 and VWF staining, Alexa Fluor 488 anti-Rat and Alexa Fluor 568 anti-Rabbit antibodies were used, respectively. To visualize smooth muscle actin staining, Alexa Fluor 555 anti-Rat antibody was used. To quantify thrombus neovascularization, PECAM/VWF double-positive cells in six high-powered fields (400 $\times$  magnification) throughout each thrombus cross section were counted. Three of the

six high-powered fields (HPFs) were from the periphery of the thrombus, and the remaining three HPFs were from the center of the thrombus (Figure S1). Alpha smooth muscle actin positive cells were counted in six high-powered fields per cross section in the same fashion.

### 2.8.5 | Quantification of calcium deposition

Two 10- $\mu\text{m}$  thick, mid-thrombus cross sections of FFPE IVC/thrombus samples were stained with Alizarin Red. Images of the IVC/thrombus cross sections were captured at 40 $\times$  magnification. ImageJ software was used to measure the fractional area of thrombus occupied by stain for calcium deposits.

## 2.9 | Statistical analysis

Data were analyzed by using GraphPad Prism statistical software.  $P < .05$  was considered significant. The following tests were used:  $\chi^2$  test, unpaired Student's  $t$  test (reported as mean  $\pm$  standard error of mean [SEM]), Mann-Whitney  $U$  test (reported as median with interquartile range [IQR]), and multiple  $t$  tests for grouped analyses (reported as mean  $\pm$  SEM).

## 3 | RESULTS

### 3.1 | Natural course of thrombus resolution and vein wall fibrosis initiation

To understand the natural course of thrombus resolution and VW remodeling in the murine IVC stenosis model of DVT, thrombus and surrounding VW were harvested from WT mice 2, 8, and 16 days postoperatively for detailed analysis (Figure S2).

#### 3.1.1 | Thrombus size decreased significantly between weeks 1 and 2 after stenosis of the IVC

Three groups of mice ( $n = 10$  per group) were operated on and monitored until tissue harvest on postoperative day 2, 8, or 16. Mice across all three groups showed statistically significant drops in baseline platelet count 24 hours after IVC stenosis ( $482 \pm 32$  vs  $908 \pm 17$   $\text{k}/\mu\text{L}$ ,  $P < .0001$ ) (Figure 1A). Thrombus incidence did not significantly differ between any groups (Figure 1B). Thrombus length and volume peaked at postoperative day 2 compared to postoperative days 8 and 16. Between postoperative day 2 and 8, no significant difference in thrombus length ( $7.2 \pm 0.9$  vs  $6.1 \pm 0.5$  mm,  $P = .2753$ ) or volume ( $18.58 \pm 3.30$  vs  $14.26 \pm 2.29$   $\text{mm}^3$ ,  $P = .2639$ ) was observed. Between postoperative day 8 and 16, however, thrombus length ( $6.1 \pm 0.5$  vs  $3.2 \pm 0.3$  mm,  $P = .0003$ ) and volume

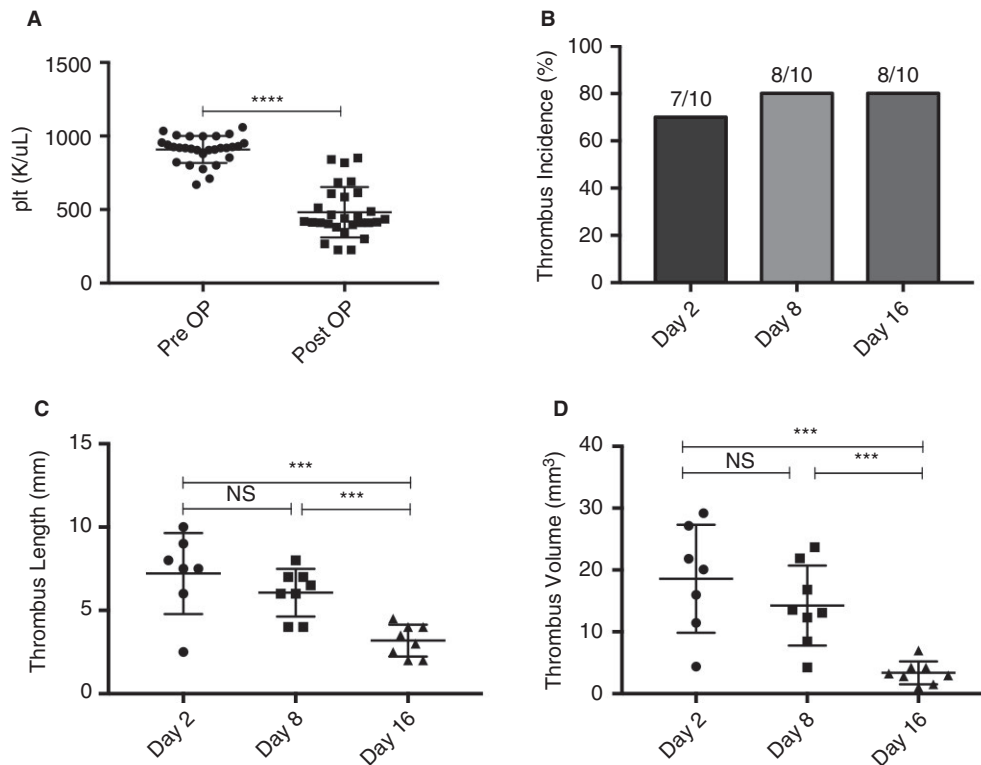


**FIGURE 1** Thrombus length and volume decrease over time in the IVC stenosis model of DVT. A, Pre- and postoperative platelet counts were measured in all mice 24 h before and 24 h after IVC stenosis surgery (n = 30). B, Thrombus incidence in mice that underwent tissue harvest on postoperative day 2 (n = 10), 8 (n = 10), or 16 (n = 10). C, Thrombus length and (D) thrombus volume on postoperative days 2, 8, and 16. Data are reported as mean  $\pm$  SEM. Unpaired, Student's t test and  $\chi^2$  test used for statistical analysis. ( $P < .05^*$ ,  $P < .01^{**}$ ,  $P < .001^{***}$ ,  $P < .0001^{****}$ )

( $14.26 \pm 2.29$  vs  $3.37 \pm 0.66$  mm<sup>3</sup>  $P = .0004$ ) decreased significantly (Figure 1C,D).

### 3.1.2 | Vein wall fibrosis begins during the first week after thrombogenesis in the murine IVC stenosis model of DVT

To determine the natural history of VW fibrosis in this mouse model of DVT, cross sections of VW and thrombi harvested from mice 2 (n = 4), 8 (n = 5), or 16 (n = 4) days after IVC stenosis were paraffin embedded and stained with Masson's Trichrome for analysis of collagen content and distribution (Figure 2A-F). VW fibrosis began as early as the first week after thrombus formation and continued to steadily increase into the second week. The VW area occupied by collagen increased between postoperative days 2 and 8 ( $2.16 \times 10^4 \pm 2.52 \times 10^3$  vs  $7.34 \times 10^4 \pm 1.83 \times 10^4$   $\mu\text{m}^2$ ,  $P = .0420$ ) and days 8 and 16 ( $7.34 \times 10^4 \pm 1.83 \times 10^4$  vs  $1.68 \times 10^5 \pm 1.42 \times 10^4$   $\mu\text{m}^2$ ,  $P = .0059$ ) (Figure 2G). There was a highly significant increase in VW collagen between days 2 and 16 ( $P = .0001$ ). Total VW area increased from postoperative days 2 to 8 ( $2.10 \times 10^5 \pm 1.32 \times 10^4$  vs  $3.36 \times 10^5 \pm 3.48 \times 10^4$   $\mu\text{m}^2$ ,  $P = .0176$ ) and from day 2 to 16 ( $2.10 \times 10^5 \pm 1.32 \times 10^4$  vs  $3.76 \times 10^5 \pm 2.96 \times 10^4$   $\mu\text{m}^2$ ,  $P = .0021$ ), but not between days 8 and 16 ( $P = .4248$ ) (Figure 2G-I).

### 3.1.3 | Thrombus fibrosis increases in the second week postoperatively while thrombus cross-sectional area decreases

Fibrosis and average cross-sectional area were examined as a proxy for thrombus maturation. Average thrombus cross-sectional area occupied by collagen increased significantly between postoperative days 8 and 16 ( $4.31 \times 10^3 \pm 1.11 \times 10^3$  vs  $3.72 \times 10^4 \pm 4.96 \times 10^3$   $\mu\text{m}^2$ ,  $P = .0002$ ) and 2 and 16 ( $3.81 \times 10^3 \pm 1.09 \times 10^3$  vs  $3.72 \times 10^4 \pm 4.96 \times 10^3$   $\mu\text{m}^2$ ,  $P = .0006$ ) but not between days 2 and 8 ( $P = .7618$ ). Average thrombus cross-sectional area decreased significantly between postoperative days 8 and 16 ( $1.96 \times 10^6 \pm 2.31 \times 10^5$  vs  $1.01 \times 10^6 \pm 2.72 \times 10^5$   $\mu\text{m}^2$ ,  $P = .0316$ ) and 2 and 16 ( $2.50 \times 10^6 \pm 3.00 \times 10^5$  vs  $1.01 \times 10^6 \pm 2.72 \times 10^5$   $\mu\text{m}^2$ ,  $P = .0103$ ) but not between days 2 and 8 ( $P = .1885$ ) (Figure 2J-L). The percent of thrombus area occupied by collagen was highest on postoperative day 16 (Figure 2L).

### 3.1.4 | Thrombus neovascularization gradually increases during the first 2 weeks after thrombogenesis in the murine IVC stenosis model of DVT

To understand the natural history of thrombus neovascularization in the murine IVC stenosis model of DVT, cross sections of VW

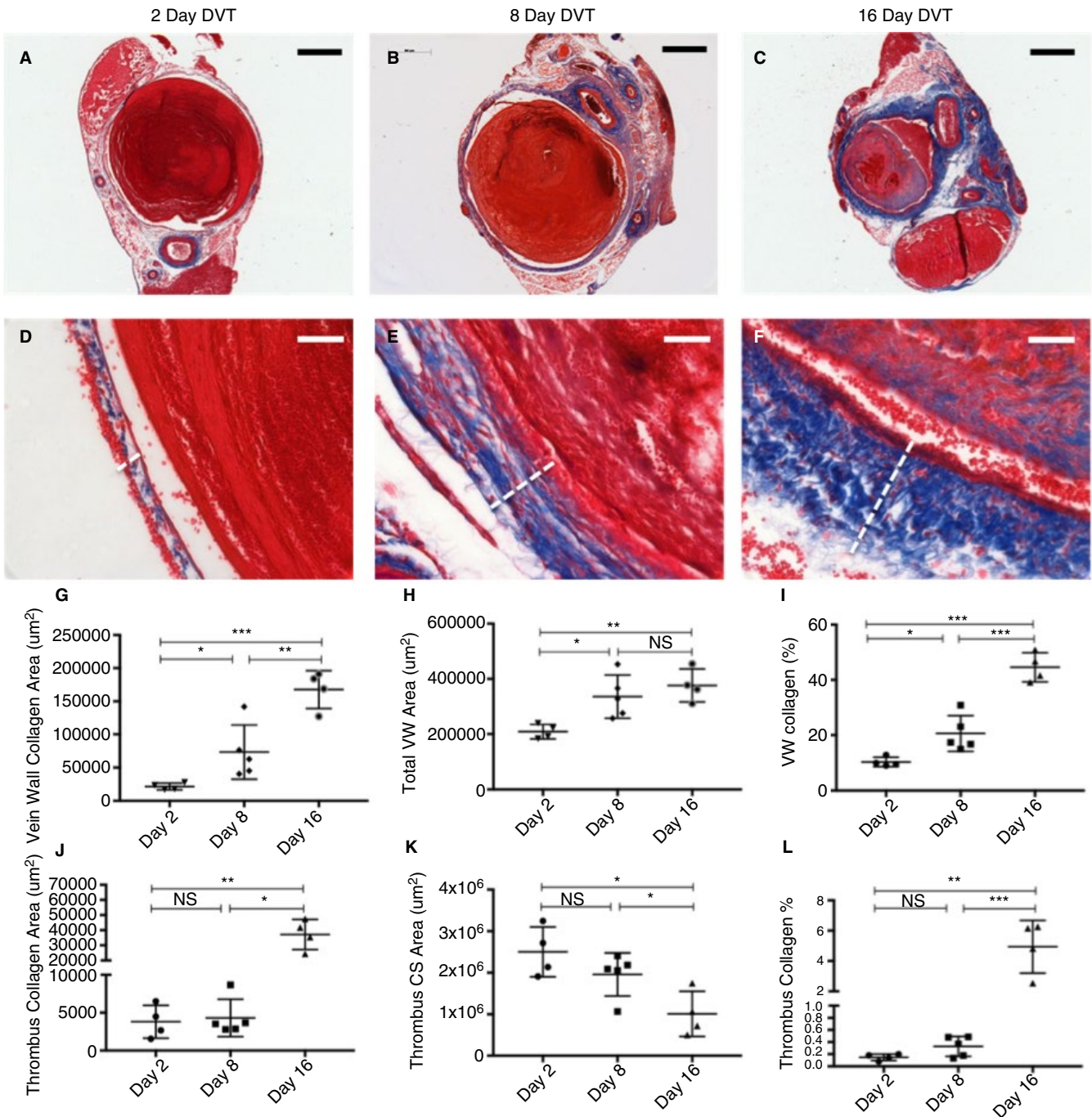


**FIGURE 2** Thrombus and vein wall fibrosis evolution over time in the IVC stenosis model of DVT. Cross sections (CS) of vein wall and thrombi harvested from mice 2 ( $n = 4$ ), 8 ( $n = 5$ ), or 16 ( $n = 4$ ) days after IVC stenosis were stained with Masson's Trichrome for analysis of collagen content and distribution. A-C, Representative low magnification (bar 500  $\mu\text{m}$ ) and D-F, high magnification (bar 50  $\mu\text{m}$ ) images of vein wall and thrombus collagen staining (white dotted line indicates vein wall thickness). G, Quantification at 2, 8, and 16 d post-stenosis of average vein wall collagen area, (H) average vein wall cross-sectional area, and (I) percent vein wall occupied by collagen. J, Quantification at 2, 8, and 16 d poststenosis of average thrombus collagen area, (K) average thrombus cross-sectional area, and (L) percent thrombus occupied by collagen. Data are reported as mean  $\pm$  SEM. Unpaired, Student's *t* test used for statistical analysis. ( $P < .05^*$ ,  $P < .01^{**}$ ,  $P < .001^{***}$ ,  $P < .0001^{****}$ ) [Colour figure can be viewed at [wileyonlinelibrary.com](http://wileyonlinelibrary.com)]

and thrombi harvested from mice 2 ( $n = 3$ ), 8 ( $n = 3$ ), or 16 ( $n = 4$ ) days after IVC stenosis were stained with immunofluorescent antibodies against endothelial markers (PECAM/CD31 and VWF) (Figure 3A-F). Thrombus neovascularization occurred, initially, at

the periphery of the thrombus, near the thrombus/VW interface (Figure 3B). As the thrombus matured, neovascular channel-like structures increased in abundance and were observed in both the periphery and the center of the thrombus (Figure 3C). PECAM/

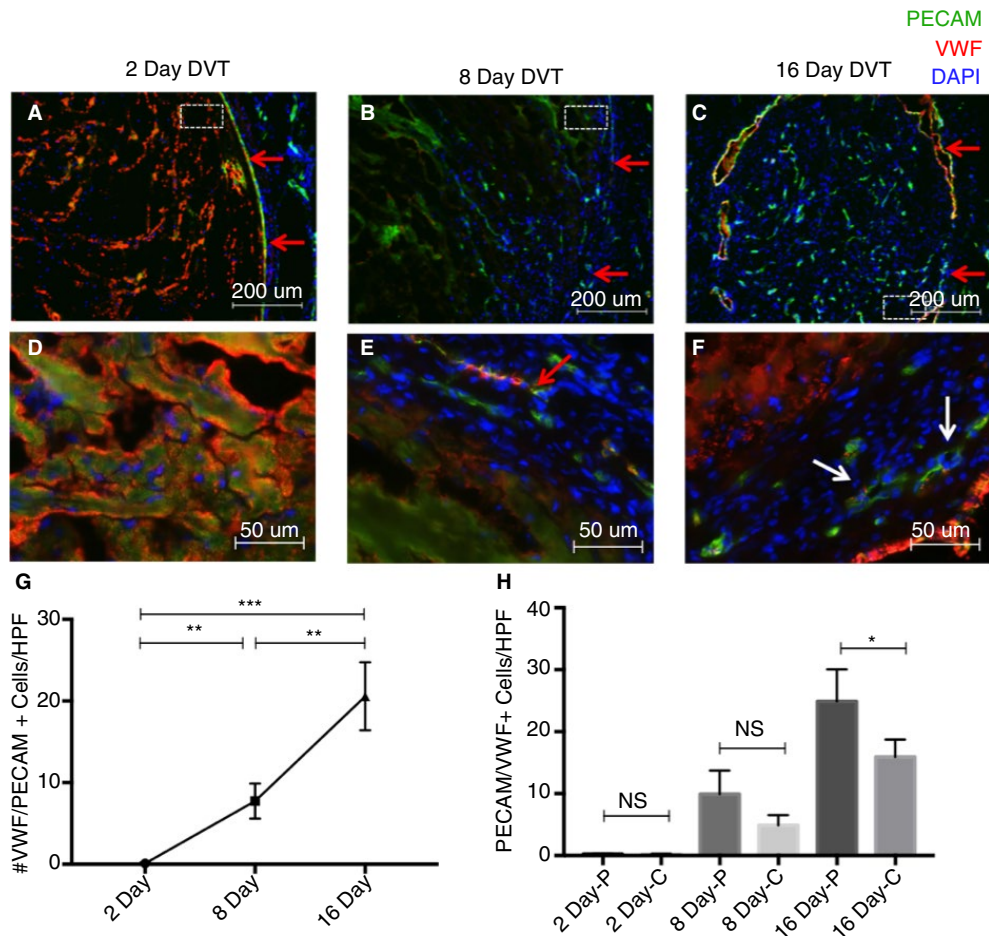


**FIGURE 3** Thrombus neovascularization over time in the IVC stenosis model of DVT. Cross sections of vein wall/thrombi harvested from mice 2 ( $n = 3$ ), 8 ( $n = 3$ ), or 16 ( $n = 4$ ) days after IVC stenosis were stained with immunofluorescent antibodies against PECAM/CD31 (488 $\lambda$ ) and VWF (568 $\lambda$ ). A-C, Representative low magnification (bar 200  $\mu\text{m}$ ) intrathrombus PECAM and VWF staining on postoperative day 2, 8, or 16 (thrombus/vein wall interface indicated by red arrows, dotted white box indicates area magnified in panel below). D-F, High magnification (bar 50  $\mu\text{m}$ ) PECAM and VWF staining at postoperative day 2, 8, or 16 in the peripheral aspect of the thrombus. G, Quantification of average number of PECAM/VWF dual-positive cells/high-powered field (HPF). Data are displayed as mean number of cells/HPF averaged across 6 HPF at 400 $\times$  magnification. H, Quantification of PECAM/VWF dual-positive cells/HPF in the peripheral (-p) vs central (-c) aspects of thrombi. Data are reported as mean  $\pm$  SEM. Unpaired, Student's *t* test used for statistical analysis. ( $P < .05^*$ ,  $P < .01^{**}$ ,  $P < .001^{***}$ ,  $P < .0001^{****}$ ) [Colour figure can be viewed at [wileyonlinelibrary.com](http://wileyonlinelibrary.com)]

VWF double-positive cells became not only more abundant in more mature thrombi but also organized into visible channels (Figure 3F). Although nearly no intrathrombus endothelial cells were observed in 2-day-old thrombi ( $9.0 \times 10^{-2} \pm 4.0 \times 10^{-2}$  cells/HPF), 8-day-old thrombi showed evidence of neovascularization ( $7.7 \pm 1.2$  cells/HPF), which steadily continued through day 16 ( $20.6 \pm 2.1$  cells/HPF). Statistically significant increases in the number of PECAM/VWF double-positive cells/HPF were observed between days 2 and 8 ( $P = .0035$ ), days 8 and 16 ( $P = .0049$ ), and days 2 and 16 ( $P = .0004$ ) (Figure 3G). At 16 days postoperatively, neovascular cells were more abundant in the thrombus periphery compared with the thrombus center ( $28.9 \pm 2.6$  vs  $15.9 \pm 1.3$  cells/HPF,  $P = .0229$ , Figure 3H).

### 3.2 | Thrombus maturation and vein wall fibrosis in platelet-depleted mice

We sought to understand the contribution of platelets to thrombus maturation, neovascularization, resolution, and VW remodeling in the period after thrombus formation. To do this, we depleted platelets in mice that had been allowed to form stable thrombi over a 2-day period. Ten days postoperatively, thrombus samples were harvested from mice depleted of platelets from postoperative days 2 through 10 or from mice treated with a control non-platelet-depleting IgG antibody for an equal duration of time. Vein wall and thrombus samples were then carefully analyzed histologically for evidence of thrombus and VW remodeling (Figure S3).

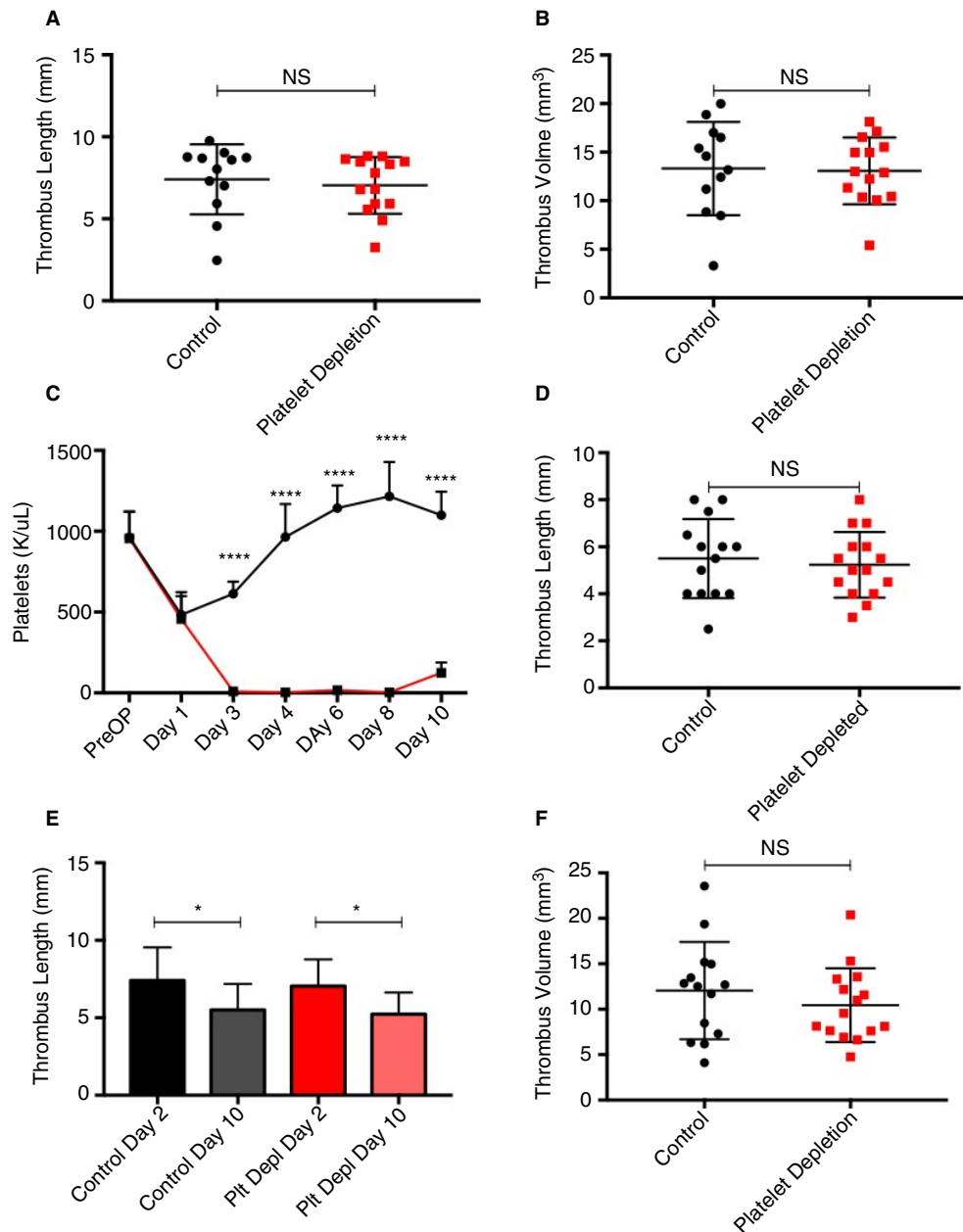


**FIGURE 4** Sustained platelet depletion after thrombogenesis does not alter thrombus length or volume. A and B, Characteristics of thrombi before antibody treatment. Thrombus length and volume 48 hours after IVC stenosis, as determined by ultrasound. C, Platelet counts in control ( $n = 14$ ) and platelet-depleted ( $n = 16$ ) mice. Surgery occurred on day 0 and platelet depletion was initiated on postoperative day 2. D, Thrombus length was measured at the time of harvest. E, Change in thrombus length over time from postoperative days 2 through 10 in control-treated and platelet-depleted mice. F, Thrombus volume at postoperative day 10. Data are reported as mean  $\pm$  SEM. Unpaired, Student's  $t$  test used for statistical analysis. ( $P < .05^*$ ,  $P < .01^{**}$ ,  $P < .001^{***}$ ,  $P < .0001^{****}$ ) [Colour figure can be viewed at [wileyonlinelibrary.com](http://wileyonlinelibrary.com)]

### 3.2.1 | Platelet depletion did not alter thrombus size

The IVC stenosis model of DVT produces thrombi under flow conditions, better mimicking the conditions under which thrombi typically form in the human body, but it has the limitation of producing thrombi of variable sizes. To prevent baseline thrombus size from being a confounding variable, we ensured that mice that would be treated with a platelet depleting or control antibody had similar thrombus sizes/platelet count drops before initiation of treatment.

Thrombus length and volume at 48 hours after IVC stenosis, as determined by ultrasound, did not differ between IgG-treated or anti-GP1b $\alpha$ -treated groups prior to starting treatment ( $7.4 \pm 0.6$  vs  $7.0 \pm 0.5$  mm,  $P = .6310$ , and  $13.32 \pm 1.39$  vs  $13.08 \pm 0.92$  mm $^3$ ,  $P = .8832$ , respectively; Figure 4A,B).

Platelet count was measured preoperatively (day -1) and on postoperative days 1, 3, 4, 6, 8, and at time of harvest on postoperative day 10. Before surgery, average platelet count did not differ between mice to be treated with control IgG ( $n = 14$ ) or

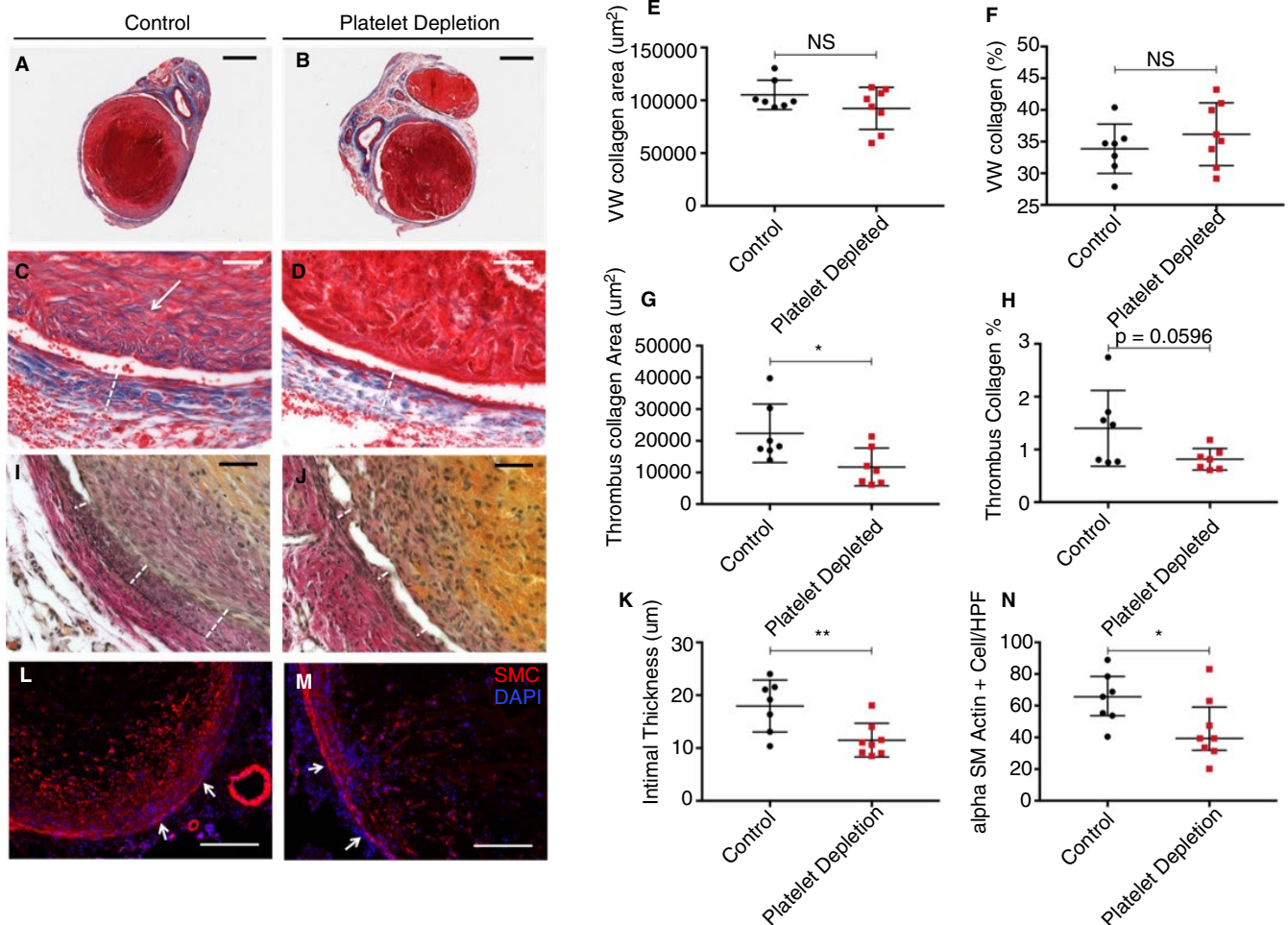


**FIGURE 5** Platelet depletion for 8 d after 2 d of thrombogenesis decreases intrathrombus collagen content, vein wall intimal thickening, and intrathrombus smooth muscle cells. Thrombus/vein wall samples from control ( $n = 7$ ) or platelet-depleted ( $n = 8$ ) mice stained for (A-D) collagen with Masson's Trichrome, (I,J) Elastic Van Gieson for elastin, and (L,M) anti- $\alpha$ SMC actin for smooth muscle cells. A-D, Representative low-magnification (bar 500  $\mu\text{m}$ ) and high-magnification (bar 50  $\mu\text{m}$ ) images of trichrome-stained tissue shown above. White arrow indicates region of intrathrombus collagen deposition, and dotted line indicates vein wall thickness. E and F, Quantification of average vein wall collagen area and percent vein wall occupied by collagen over time. G-H, Quantification of average thrombus collagen area and percent thrombus occupied by collagen. I and J, Images of Van Gieson stained thrombus/vein wall cross sections at high magnification (bar 50  $\mu\text{m}$ ). Images shown above are representative of cohort (white dotted line indicates intimal thickness). K, Quantification of intimal thickness in mice treated with platelet-depleting antibody or control IgG. L and M, Representative low-magnification (bar 200  $\mu\text{m}$ ) images of smooth muscle (red) and DAPI (blue) staining in thrombi from control and platelet-depleted mice. White arrows indicate the approximate borders of the thrombus/vein wall interface, coming from the vein wall pointing toward the thrombus. N, Quantification of intrathrombus smooth muscle cell staining, performed across 6 HPF at 400 $\times$ . Data are shown as mean  $\pm$  SEM (E-H) or median with IQR (K-N). Unpaired, Student's  $t$  test (E-H) or Mann-Whitney  $U$  test (K-N) were used for statistical analysis. ( $P < .05^*$ ,  $P < .01^{**}$ ,  $P < .001^{***}$ ,  $P < .0001^{****}$ ) [Colour figure can be viewed at [wileyonlinelibrary.com](http://wileyonlinelibrary.com)]

platelet-depleting antibody ( $n = 16$ ) ( $963 \pm 45$  vs  $956 \pm 43$  K/ $\mu\text{L}$ ,  $P = .9087$ ). Platelet counts also did not differ between mice to be treated with control or platelet-depleting antibody on postoperative day 1, before the initiation of control treatment or platelet depletion ( $483 \pm 39$  vs  $457 \pm 36$  K/ $\mu\text{L}$ ,  $P = .6268$ ) (Figure 4C). Statistically significant platelet depletion was successfully maintained by daily injections of platelet-depleting antibody from postoperative day 2 to postoperative day 10 (Figure 4C,  $P < .001$ ). Mouse weight was monitored daily. All mice experienced a drop in baseline body weight on postoperative day 1, which gradually increased toward baseline over the course of 1.5 weeks. No statistically significant differences

in body weight were detected in platelet-depleted and control antibody-treated mice (Figure S4).

On postoperative day 10, mice were sacrificed for IVC/thrombus harvest. Thrombus length was measured at time of harvest, and thrombus volume calculated as described in the Methods section. On postoperative day 10, thrombus length did not differ between platelet-depleted and control-treated mice ( $5.2 \pm 0.4$  vs  $5.5 \pm 0.5$  mm,  $P = .6447$ , Figure 4D). Statistically significant reductions in thrombus length between postoperative days 2 and 10 were observed in both control-treated ( $7.4 \pm 0.6$  vs  $5.5 \pm 0.5$  mm,  $P = .0175$ ) and platelet-depleted ( $7.0 \pm 0.5$  vs  $5.2 \pm 0.4$  mm,

$P = .0045$ ) mice. A similar decrease in thrombus length from postoperative day 2 to postoperative day 10 was observed in platelet-depleted (25% reduction in thrombus length) and control-treated (23% reduction in thrombus length) mice (Figure 4E). Thrombus volume on postoperative day 10 also did not differ between platelet-depleted and control-treated mice ( $10.45 \pm 1.05$  vs  $12.05 \pm 1.43$  mm<sup>3</sup>,  $P = .3701$ ) (Figure 4F).

### 3.2.2 | Platelet depletion decreases thrombus fibrosis, vein wall intimal thickness, and intrathrombus smooth muscle cell invasion

Images of trichrome stained thrombus/VW cross sections from platelet depleted ( $n = 8$ ) and control-treated mice ( $n = 7$ ) were captured at low and high magnification (Figure 5A-D). Mice treated with platelet-depleting antibody had similar VW collagen area and percentages of VW occupied by collagen compared with control-treated mice ( $9.23 \times 10^4 \pm 7.04 \times 10^3$  vs  $1.05 \times 10^5 \pm 5.25 \times 10^3$  μm<sup>2</sup>,  $P = .1766$  &  $36.2 \pm 1.6$  vs  $33.9 \pm 1.5\%$ ,  $P = .3405$ , respectively) (Figure 5E-F). However, mice treated with platelet-depleting antibody had significantly lower intrathrombus collagen areas compared with controls ( $11.74 \times 10^4 \pm 2.26 \times 10^3$  vs  $2.24 \times 10^4 \pm 3.49 \times 10^3$  μm<sup>2</sup>,  $P = .0251$ ) and a strong trend toward decreased percentage of thrombus occupied by collagen ( $0.8 \pm 0.1$  vs  $1.4 \pm 0.3\%$ ,  $P = .0596$ , Figure 5G-H). In parallel, we also analyzed tissue sections for evidence of calcification. Postthrombotic VW calcium deposition was not detected. Thrombus calcification was observed in control and platelet-depleted mice, with no difference in calcium deposition between control and platelet-depleted mice (Figure 5S).

Van Gieson staining identified the elastic lamina within the vein and, therefore, helped to delineate the thickness of the intima. Images of Van Gieson stained thrombus/VW cross sections were captured at high magnification (Figure 5I,J). A reduction in intimal thickening was observed in platelet-depleted mice ( $n = 8$ ) compared with controls ( $n = 7$ ) ( $11.5 \pm 1.1$  vs  $17.9 \pm 1.9$  mm,  $P = .0092$ ) (Figure 5K).

Cross sections of VWs and thrombi harvested from platelet-depleted ( $n = 8$ ) or control ( $n = 7$ ) mice 10 days after IVC stenosis were stained with an immunofluorescent antibody against alpha smooth muscle actin (Figure 5L,M). In thrombi from both groups of mice, robust smooth muscle staining was observed in the periphery of the thrombus, with decreased smooth muscle cell staining in the center of the thrombus. A decrease in total intrathrombus smooth muscle cell invasion was observed in thrombi harvested from platelet-depleted mice compared with those harvested from control mice (median 39.1, IQR 31.9-59.1 vs 65.6, IQR 53.7-78.4 cells/HPF,  $P = .0401$ ) (Figure 5N).

Vascular smooth muscle cells are known to infiltrate resolving thrombi and line neo-vessels. To examine the role of platelets in thrombus neovascularization, cross sections of VW and thrombi harvested from platelet-depleted ( $n = 8$ ) or control ( $n = 7$ ) mice 10 days after IVC stenosis were stained with immunofluorescent

antibodies against endothelial markers (PECAM/CD31 and VWF) (Figure S6). Although the median of endothelial cells in thrombi from platelet depleted mice was half the number of that observed in control mice, the difference was not statistically significant (median 7.6, IQR 4.9-15.3 vs 17.6, IQR 9.4-21.7 cells/HPF,  $P = .0939$ , Figure S6).

## 4 | DISCUSSION

Almost one-half of patients with proximal DVT may go on to develop PTS despite anticoagulation therapy.<sup>37</sup> Characterized by edema, swelling, chronic leg pain, leg heaviness, skin changes, and ulcerations, PTS is associated with a significantly decreased quality of life, in addition to substantial health care costs.<sup>1,10,37,38</sup> Hallmarks of PTS include venous reflux and hypertension, VW fibrosis, and neointimal hyperplasia. Given the significant impact of PTS on patient quality of life and disability, finding therapies that can prevent or lessen the severity of PTS is of the utmost importance.

This study was performed to determine the role of platelets in thrombus maturation, resolution, and postthrombotic VW remodeling. We found that circulating platelets play an important role in directing the cellular organization of resolving thrombi. Platelet depletion decreased thrombus fibrosis and smooth muscle cell invasion, while still allowing for a normal reduction in thrombus size over time. Importantly, platelet depletion decreased VW intimal thickening, a recognized histological feature associated with PTS.<sup>6</sup>

Overall, platelet depletion was well tolerated by mice, despite our initial concerns regarding thrombocytopenia in the setting of a recent operation and DVT, injurious, and inflammatory events.<sup>39-42</sup> Studies have shown that thrombocytopenia alone does not result in spontaneous hemorrhage in mice, but that thrombocytopenia in the setting of an inflammatory event (eg, lung irritation, dermatitis, stroke) results in hemorrhage. In mouse models of DVT, markers of both local and systemic inflammation peak at 6 hours after surgery and are significantly reduced 48 hours postoperatively.<sup>40,41</sup> Our laboratory has previously shown that depleting platelets after such DVT surgery does not cause excessive bleeding.<sup>35</sup> Initiating platelet depletion after peak thrombus size is reached at 48 hours helped to avoid bleeding; we narrowed our study to the effect of circulating platelets on an established thrombus, therefore avoiding the confounding variable of altering thrombogenesis, a process in which platelets are known to play a critical role.<sup>29,35,43,44</sup> Although the mechanisms by which platelets drive smooth muscle cell invasion, thrombus fibrosis, and VW intimal hyperplasia were not explored in this initial study, with these preliminary data and an understanding of platelet physiology, we can begin to generate several mechanistic hypotheses, which will require future investigation. Platelets are rich in TGF-β, a known regulator of extracellular matrix secretion and pro-fibrotic growth factor.<sup>7,16,27,45-49</sup> TGF-β requires activation, but the factors that mediate its activation, including plasmin and matrix metalloproteinases, are all locally found within the thrombus environment.<sup>7,45</sup> Although TGF-β function is dependent on the receptor

subtype with which it interacts, vascular lesions have been shown to be rich in type II TGF- $\beta$  receptors, which when activated, promote ECM production.<sup>7,46</sup> Furthermore, soluble TGF- $\beta$  inhibition has been shown to decrease fibrosis in vascular lesions, although it should be noted that these studies were carried out in arterial, as opposed to venous, vascular lesions.<sup>48</sup> We speculate that the decrease in thrombus fibrosis observed in platelet-depleted mice could potentially be due to decreased delivery of platelet-derived TGF- $\beta$ .

Although collagen deposition occurs naturally during DVT resolution and wound healing, excessive collagen deposition, known as fibrosis, can be detrimental to the healing process.<sup>16</sup> That thrombus fibrosis can be reduced by platelet depletion is a novel and exciting finding. A less fibrotic thrombus may be easier to pharmacomechanically lyse and may pose less of a threat to the VW, as thrombi are incorporated into the VW during the process of resolution, and smooth muscle cells may even proliferate after this.<sup>50-52</sup> Along with a significant decrease in intrathrombus collagen, a significant decrease in smooth muscle cell invasion into the thrombus was also observed in platelet-depleted mice. Platelets are known to contain several growth factors that can direct vascular smooth muscle cell activity, including TGF- $\beta$ , basic fibroblast growth factor (bFGF), and platelet-derived growth factor (PDGF), all of which have been identified as key regulators of vascular smooth muscle cell migration, proliferation, and phenotype.<sup>7,27,34</sup> We, therefore, speculate that reductions in platelet-derived TGF- $\beta$ , bFGF, and PDGF in anti-GP1b $\alpha$ -treated mice may be responsible for the decrease in smooth muscle cell invasion into resolving thrombi.

Long ago, our laboratory showed that circulating platelets promote angiogenesis and prevent bleeding of angiogenic vessels both in healthy tissue and in tumors.<sup>31,53</sup> Thrombus neovascularization is consistently observed during thrombus resolution in both human DVT and mouse models of DVT.<sup>15,18,22</sup> As venous thrombi mature, cells with endothelial characteristics (CD31<sup>+</sup>, VWF<sup>+</sup>, laminin, and smooth muscle cell lined) appear within the body of the thrombus.<sup>9,18,19,22,54</sup> These neovascular channels are thought to contribute to lumen recanalization, although their exact role in thrombus resolution remains debated.<sup>19,20,22,23,54,55</sup> Anticipating that neovascularization would follow smooth muscle cell infiltration and matrix deposition, we hypothesized that platelet-depleted mice would have fewer neovascular cells within thrombi than their control-treated peers. Although we observed a weak trend toward decreased thrombus neovascularization in platelet-depleted mice, a statistically significant reduction in thrombus neovascularization was not achieved. This may be due to significant variation between animals, analyzing a timepoint too early in thrombus resolution, or lack of effect. Analyzing a later timepoint in thrombus resolution (ie, 3-4 weeks) would be an ideal subsequent study; however, we were limited by the number of days platelet-depleting antibody can be administered before an immune response is mounted and platelet depletion is no longer effective. Although a reduction in thrombus neovascularization was not demonstrated in platelet-depleted mice, this study produced a valuable finding for the field of angiogenesis research. The IVC stenosis model of DVT in WT mice represents a model of

naturally occurring angiogenesis that is not induced by injection of growth factors, such as bFGF, into artificial tissue (ie, Matrigel) or tissues that usually are devoid of blood vessels (ie, cornea, bead implantation model). A pilot study from our laboratory involving systemic India ink perfusion at time of death in mice 10 days after IVC stenosis showed India ink within neovascular channels of the thrombus, suggesting that these neovascular channels participate in systemic circulation. This pilot study was, however, underpowered, and additional mice should be added in the future to draw meaningful conclusions. IVC stenosis produces tissue that will naturally become vascularized, and this process can be inhibited, enhanced, and quantified. Thus, this model provides an opportunity to examine the efficacy of anti- or pro-angiogenic drugs in a natural setting.

Importantly, we have shown that intimal thickening was reduced in platelet-depleted mice compared with control treated mice. Intimal thickening or neointimal hyperplasia, characterized by the invasion of smooth muscle cells from the vessel media and excessive extracellular matrix deposition, is one of the hallmarks of adverse post-thrombotic VW change.<sup>6,56,57</sup> Evidence exists that in the setting of both arterial and venous endothelial injury, as occurs during arterial angioplasty and vein harvest for bypass, platelets accumulate on injured endothelium and drive neo-intimal hyperplasia.<sup>58</sup> Platelet adhesion to VWF, and subsequent activation and secretion of factors such as PDGF, bFGF, and TGF- $\beta$ , all drivers of smooth muscle chemotaxis and proliferation, are suspected to play an important role in intimal neoplasia after vessel injury.<sup>56,57,59</sup> We now show that, even in a model of DVT produced without physical injury to the endothelium, circulating platelets impact intimal neoplasia. Our study indicates that further investigation into the role of platelets in post-thrombotic syndrome is merited.

This study is not without limitations. The 10-day time point after IVC stenosis fails to capture the final endpoint of VW remodeling after complete thrombus resolution. In the mouse IVC stenosis model of DVT, complete or near-complete thrombus resolution typically is achieved 3 to 4 weeks after thrombogenesis. This time point was not examined because of the inability to maintain antibody-mediated platelet depletion in mice for several weeks. Future studies that aim to characterize the mechanism by which platelet depletion decreases thrombus smooth muscle cell invasion, fibrosis, and VW intimal thickening should be performed, and the impact of platelet depletion on platelet burden within the thrombus established.

In conclusion, we found that platelet depletion after thrombogenesis fundamentally alters thrombus maturation and postthrombotic VW remodeling. Thrombocytopenic mice had less fibrotic thrombi, with fewer invading smooth muscle cells, and VWs that showed less intimal thickening. These findings are both significant and clinically relevant. Decreasing thrombus fibrosis may make the thrombus easier for the body to naturally resorb and has the potential to improve pharmacological thrombolysis or surgical thrombus removal. We also found that intimal thickening is reduced by platelet depletion after the formation of DVT. Preventing intimal thickening by inhibition of platelet recruitment after DVT has the potential to lessen the severity of PTS, a serious side effect of venous thrombosis. Once it is

determined what factors within platelets or what platelet-substrate interactions are responsible for driving thrombus fibrosis, smooth muscle cell invasion, and vein wall intimal thickening, we can target these molecular actors in the treatment of DVT.

## ACKNOWLEDGMENTS

The following funding agencies must be acknowledged for their generous financial support of this project: The National Heart, Lung and Blood Institute (R35 HL135765 grant to D.D.W.), The American Heart Association, Founders Affiliate Medical Student Research Fellowship Award; The Society for Vascular Surgery, Medical Student Research Fellowship Award; and The American Society of Hematology, HONORs Award to E.D.R.. We thank Dr Thomas Wakefield and his laboratory for their support, Boston Children's Hospital KARP Animal Facilities staff for their advice, and Tiffany Frary for help in the preparation of the manuscript.

## CONFLICT OF INTEREST

Dr. Wagner is on the Scientific Advisory Board of Neutrolis, a pre-clinical-stage biotech company focused on DNases. The remaining authors have no conflicts of interest to disclose.

## AUTHOR CONTRIBUTION

Elise DeRoo undertook primary experiment design, execution of experiments including small animal surgeries, tissue harvest and processing, data analysis, and manuscript authorship/revision. Kimberly Martinod assisted in teaching the IVC stenosis model of VT in mice and furthermore contributed to primary experiment concept/design, data analysis, and manuscript review/editing. Deya Cherpokova contributed to primary experiment design, assisted with animal care postoperatively, data analysis, and contributed to manuscript review/editing. Tobias Fuchs performed the initial platelet depletion in VT studies in mice, gathering the preliminary data that formed the basis for this study and furthermore contributed to manuscript review/editing. Stephen Cifuni, Wagner Laboratory manager, contributing by managing the Wagner division of the KARP animal facility, and ensuring all necessary equipment/supplies were available to execute the previously described experiments and furthermore contributed to manuscript review/editing. Long Chu and Caleb Staudinger, Wagner Laboratory techs, assisted in the management of the KARP animal facility and tissue processing and to manuscript review/editing. Denisa D. Wagner, principal investigator, contributed substantially to experiment concept, design, data analysis/interpretation, and manuscript preparation.

## ORCID

Elise DeRoo  <https://orcid.org/0000-0003-1440-317X>

Kimberly Martinod  <https://orcid.org/0000-0002-1026-6107>

Denisa D. Wagner  <https://orcid.org/0000-0002-4494-413X>

## REFERENCES

- Benjamin EJ, Muntner P, Alonso A, et al. Heart disease and stroke statistics—2017 update: a report from the American Heart Association. *Circulation*. 2017;135:e146–e603.
- Bartholomew JR. Update on the prevention of venous thromboembolism. *Cleve Clin J Med*. 2017;84:39–46.
- Kearon C. Natural history of venous thromboembolism. *Circulation*. 2003;107:22–31.
- Goldhaber SZ, Buring JE, Lipnick RJ, Hennekens CH. Pooled analyses of randomized trials of streptokinase and heparin in phlebographically documented acute deep venous thrombosis. *Am J Med*. 1984;76:393–397.
- Vedantham S, Goldhaber SZ, Julian JA, et al. Pharmacomechanical catheter-directed thrombolysis for deep-vein thrombosis. *N Engl J Med*. 2017;377:2240–2252.
- Wojcik BM, Wroblewski SK, Hawley AE, Wakefield TW, Myers DD, Diaz JA. Interleukin-6: a potential target for post-thrombotic syndrome. *Ann Vasc Surg*. 2011;25:229–239.
- DeRoo S, Deatrck KB, Henke PK. The vessel wall: a forgotten player in post thrombotic syndrome. *Thromb Haemost*. 2010;104:681–692.
- Deatrck KB, Eliason JL, Lynch EM, et al. Vein wall remodeling after deep vein thrombosis involves matrix metalloproteinases and late fibrosis in a mouse model. *J Vasc Surg*. 2005;42:140–148.
- Henke PK, Varma Manu, Deatrck K, et al. Neutrophils modulate post-thrombotic vein wall remodeling but not thrombus neovascularization. *Thromb Haemost*. 2006;95:272–281.
- Farrell JJ, Sutter C, Tavri S, Patel I. Incidence and interventions for post-thrombotic syndrome. *Cardiovasc Diagn Ther*. 2016;6:623–631.
- Van Rij AM, Hill G, Krysa J, et al. Prospective study of natural history of deep vein thrombosis: early predictors of poor late outcomes. *Ann Vasc Surg*. 2013;27:924–931.
- Nayak L, Vedantham S. Multifaceted management of the post-thrombotic syndrome. *Semin Intervent Radiol*. 2012;29:16–22.
- Kahn SR, Ginsberg JS. Relationship between deep venous thrombosis and the postthrombotic syndrome. *Arch Intern Med*. 2004;164:17–26.
- Sevitt S. The mechanisms of canalisation in deep vein thrombosis. *J Pathol*. 1973;110:153–165.
- Sevitt S. The vascularisation of deep-vein thrombi and their fibrous residue: a post-mortem angiographic study. *J Pathol*. 1973;111:1–11.
- Diegelmann RF, Evans MC. Wound healing: an overview of acute, fibrotic and delayed healing. *Front Biosci*. 2004;9:283–289.
- Meissner MH, Zierler BK, Bergelin RO, Chandler WL, Strandness DE. Coagulation, fibrinolysis, and recanalization after acute deep venous thrombosis. *J Vasc Surg*. 2002;35:278–284.
- Wakefield TW, Linn MJ, Henke PK, et al. Neovascularization during venous thrombosis organization: a preliminary study. *J Vasc Surg*. 1999;30:885–893.
- Henke PK, Wakefield TW, Kadell AM, et al. Interleukin-8 administration enhances venous thrombosis resolution in a rat model. *J Surg Res*. 2001;99:84–91.
- Henke PK, Varga A, De S, et al. Deep vein thrombosis resolution is modulated by monocyte CXCR2-mediated activity in a mouse model. *Arterioscler Thromb Vasc Biol*. 2004;24:1130–1137.
- Leu HJ, Feigl W, Susani M. Angiogenesis from mononuclear cells in thrombi. *Virchows Arch A Pathol Anat Histopathol*. 1987;411:5–14.
- Modarai B, Burnand KG, Humphries J, Waltham M, Smith A. The role of neovascularisation in the resolution of venous thrombus. *Thromb Haemost*. 2005;93:801–809.
- Modarai B, Burnand KG, Sawyer B, Smith A. Endothelial progenitor cells are recruited into resolving venous thrombi. *Circulation*. 2005;111:2645–2653.
- Diaz JA, Obi AT, Myers DD, et al. Critical review of mouse models of venous thrombosis. *Arterioscler Thromb Vasc Biol*. 2012;32:556–562.
- Varma MR, Varga AJ, Knipp BS, et al. Neutropenia impairs venous thrombosis resolution in the rat. *J Vasc Surg*. 2003;38:1090–1098.
- Shantsila E, Lip GYH. The role of monocytes in thrombotic disorders: Insights from tissue factor, monocyte-platelet aggregates and novel mechanisms. *Thromb Haemost*. 2009;102:916–924.

27. Crooks MG, Fahim A, Naseem KM, Morice AH, Hart SP. Increased platelet reactivity in idiopathic pulmonary fibrosis is mediated by a plasma factor. *PLoS ONE*. 2014;9:1-8.
28. O'Sullivan BP, Michelson AD. The inflammatory role of platelets in cystic fibrosis. *Am J Respir Crit Care Med*. 2006;173:483-490.
29. Van Der Meijden PE, Heemskerk J, Hamulya K. Classification of Venous Thromboembolism (VTE). *J Thromb Haemost*. 2005;3:2575-2577.
30. Pipili-Synetos E, Papadimitriou E, Maragoudakis ME. Evidence that platelets promote tube formation by endothelial cells on matrigel. *Br J Pharmacol*. 1998;125:1252-1257.
31. Kisucka J, Butterfield CE, Duda DG, et al. Platelets and platelet adhesion support angiogenesis while preventing excessive hemorrhage. *Proc Natl Acad Sci*. 2006;103:855-860.
32. Sabrkhany S, Griffioen AW, Oude Egbrink MGA. The role of blood platelets in tumor angiogenesis. *Biochim Biophys Acta*. 2011;1815:189-196.
33. Di Vito C, Navone SE, Marfia G, et al. Platelets from glioblastoma patients promote angiogenesis of tumor endothelial cells and exhibit increased VEGF content and release. *Platelets*. 2017;28:585-594.
34. Brill A, Elinav H, Varon D. Differential role of platelet granular mediators in angiogenesis. *Cardiovasc Res*. 2004;63:226-235.
35. von Brühl M-L, Stark K, Stainhart A, et al. Monocytes, neutrophils, and platelets cooperate to initiate and propagate venous thrombosis in mice in vivo. *J Exp Med*. 2012;209:819-835.
36. Martinod K, Demers M, Fuchs TA, et al. Neutrophil histone modification by peptidylarginine deiminase 4 is critical for deep vein thrombosis in mice. *PNAS*. 2013;110:8674-8679.
37. Baldwin MJ, Moore HM, Rudarakanchana N, Gohel M, Davies AH. Post-thrombotic syndrome: a clinical review. *J Thromb Haemost*. 2013;11:795-805.
38. Kahn S, Ducruet T, Lamping DL, et al. Prospective evaluation of health-related quality of life in patients with deep venous thrombosis. *Arch Intern Med*. 2005;165:1173.
39. Rodriguez AL, Wojcik BM, Wroblewski SK, Myers DD, Wakefield TW, Diaz JA. Statins, inflammation and deep vein thrombosis: a systematic review. *J Thromb Thrombolysis*. 2012;33:371-382.
40. Hish GA, Diaz JA, Hawley AE, Myers DD, Lester PA. Effects of analgesic use on inflammation and hematology in a murine model of venous thrombosis. *J Am Assoc Lab Anim Sci*. 2014;53:485-493.
41. Patterson KA, Zhang X, Wroblewski SK, et al. Rosuvastatin reduced deep vein thrombosis in ApoE gene deleted mice with hyperlipidemia through non-lipid lowering effects. *Thromb Res*. 2013;131:268-276.
42. Goerge T, Ho-Tin-Noe B, Carbo C, et al. Inflammation induces hemorrhage in thrombocytopenia. *Blood*. 2008;111:4958-4964.
43. Brill A, Fuchs TA, Chauhan AK, et al. von Willebrand factor-mediated platelet adhesion is critical for deep vein thrombosis in mouse models. *Blood*. 2011;117:1400-1407.
44. Heemskerk JWM, Bevers EM, Lindhout T. Platelet activation and blood coagulation. *Thromb Haemost*. 2002;88:186-193.
45. Annes JP, Munger JS, Rifkin DB. Making sense of latent TGF $\beta$  activation. *J Cell Sci*. 2003;116:217-224.
46. McCaffrey TA, Consigli S, Du B, et al. Decreased type II/Type I TGF- $\beta$  receptor ratio in cells derived from human atherosclerotic lesions. *J Clin Invest*. 1999;96:2667-2675.
47. Meyer A, Wang W, Qu J, et al. Platelet TGF  $\beta$  contributions to plasma TGF  $\beta$ , cardiac fibrosis, and systolic dysfunction in a mouse model of pressure overload. *Blood*. 2012;119:1064-1074.
48. Lutgens E, Gijbels M, Smook M, et al. Transforming growth factor- $\beta$  mediates balance between inflammation and fibrosis during plaque progression. *Arterioscler Thromb Vasc Biol*. 2002;22:975-982.
49. Martinod K, Witsch T, Erpenbeck L, et al. Peptidylarginine deiminase 4 promotes age-related organ fibrosis. *J Exp Med*. 2017;214:439-458.
50. Chrysanthopoulou A, Mitroulis I, Apostolidou E, et al. Neutrophil extracellular traps promote differentiation and function of fibroblasts. *J Pathol*. 2014;233(3):294-307. <https://doi.org/10.1002/path.4359>
51. Humphries J, McGuinness CL, Smith A, Waltham M, Poston R, Burnand KG. Monocyte chemotactic protein-1 (MCP-1) accelerates the organization and resolution of venous thrombi. *J Vasc Surg*. 1999;30:894-900.
52. Morris TA. Natural history of venous thromboembolism. *Crit Care Clin*. 2011;27:869-884.
53. Ho-Tin B, Demers M, Wagner D. How platelets safeguard vascular integrity. *J Thromb Haemost*. 2011;9:56-65.
54. Varma MR, Moaveni DM, Dewyer NA, et al. Deep vein thrombosis resolution is not accelerated with increased neovascularization. *J Vasc Surg*. 2004;40:536-542.
55. Modarai B, Humphries J, Burnand KG, et al. Adenovirus-mediated VEGF gene therapy enhances venous thrombus recanalization and resolution. *Arterioscler Thromb Vasc Biol*. 2008;28:1753-1759.
56. Liu MW, Roubin GS, King SB. Restenosis after coronary angioplasty: potential biologic determinants and role of intimal hyperplasia. *Circulation*. 1989;79:1374-1387.
57. Roy-Chaudhury P, Kelly BS, Miller MA, et al. Venous neointimal hyperplasia in polytetrafluoroethylene dialysis grafts. *Kidney Int*. 2001;59:2325-2334.
58. Cassar K, Bachoo P, Brittenden J. The role of platelets in peripheral vascular disease. *Eur J Vasc Endovasc Surg*. 2003;25:6-15.
59. Witsch T, Martinod K, Sorvillo N, et al. Recombinant human ADAMTS13 treatment improves myocardial remodeling and functionality after pressure overload injury in mice. *J Am Heart Assoc*. 2018;7:e007004.

## SUPPORTING INFORMATION

Additional supporting information may be found online in the Supporting Information section.

**How to cite this article:** DeRoo E, Martinod K, Cherpokova D, et al. The role of platelets in thrombus fibrosis and vessel wall remodeling after venous thrombosis. *J Thromb Haemost*. 2021;19:387-399. <https://doi.org/10.1111/jth.15134>